Intermodulation Distortion Analysis of MESFET Amplifiers Using the Volterra Series Representation

ROBERT ARAM MINASIAN

Abstract—**Third-order intermodulation distortion generated in a MESFET amplifier is analyzed by means of the Volterra series representation. A transistor model is used which enables direct analytical determination of the nonlinear elements from small-signal measurements. The four nonlinearities considered are the gate capacitance, transconductance, drain feedback capacitance, and output conductance. Volterra transfer functions are derived for a simplified model and closed-form expressions for the third-order intermodulation ratio and intercept point are determined. The equations show the dependence of distortion on frequency, terminating impedances, and transistor parameters. Principal sources of distortion are identified and the influence of device parameters and network terminations is investigated. Experimental verification on specific MESFET amplifiers, with 2-μm and 1-μm gate devices, comparing predicted and measured intermodulation products for various load conditions is presented.**

I. Introduction

THE MICROWAVE GaAs MESFET has found application in wideband highly linear power amplifiers [1], [2]. In communication systems, the device intermodulation characteristic becomes an important consideration. This paper investigates distortion in MESFET amplifiers using simple nonlinear device models which are analyzed by a systematic procedure based on the Volterra series or nonlinear transfer function approach. The Volterra series expansion allows a detailed representation of device characteristics including reactive effects. Since its original application to the analysis of nonlinear networks [3], the technique has been used to investigate high-frequency distortion in a variety of devices [4]–[10].

The intermodulation characteristics of MESFET's have been studied recently [11]–[14]. These analyses employ simple power series descriptions which rely on an *a priori* knowledge of the controlling voltage. As well, they are simplified with regard to input nonlinearities and ignore the effects of out-of-band terminations. This paper presents a more general analysis procedure based on the Volterra series, which includes interactions between the nonlinear parameters and spectral components at intermodulation and harmonic frequencies. The analysis may readily be extended to more complex networks involving multistage amplifiers. The transistor models used, incorporating gate, transconductance, and drain nonlinearities, have physical origins and are directly deduced from small-signal measurements. A third-order analysis is performed which applies for small-to-moderate signal levels prior to the onset of gain saturation. Closed-form expressions for third-order intermodulation distortion ratio and intercept point are derived which reveal the dominant sources of distortion and its dependence on parameters of the MESFET. As well, investigations on the sensitivity to out-of-band terminations are carried out. The approach taken is to perform a computer Volterra analysis of the nonlinear amplifier equivalent circuit (denoted as Model A) and then to analyze a simplified, related circuit (denoted as Model B) which enables the derivation of tractable closed-form expressions for distortion. The analytical results are compared mutually, and against measurements on two experimental MESFET amplifiers, employing a 2-μm and a 1-μm gate-length device, and the influence of device parameters and terminations is examined.

Manuscript received August 2, 1978; revised January 2, 1979. This work was supported by the Australian Radio Research Board.

The author is with the Department of Electrical Engineering, University of Melbourne, Parkville, Victoria, 3052, Australia.

II. MESFET Amplifier Models

A. Model A

The nonlinear circuit representation of the MESFET amplifier is shown in Fig. 1. It consists of an input signal source $v_s(t)$ with source impedance $Z_G(f)$, the transistor, and a load impedance $Z_L(f)$. The large-signal equivalent circuit for the MESFET is based on the model developed in [16]. Four dominant nonlinearities arising from the voltage-dependent intrinsic elements are considered: the Schottky-barrier junction capacitance at the gate, the transconductance, the feedback capacitance, and the drain conductance. The nonlinear characteristics of these elements are directly and conveniently determined from small-signal s-parameter measurements over a range of bias points [15], [16]. This model, in conjunction with the quasi-static assumption which allows extension to the dynamic nonlinear case, has been found to be capable of good results in predicting distortion products [16].

B. Model B

The simplified nonlinear model used in deriving closed-form expressions for intermodulation distortion is shown in Fig. 2. The feedback capacitance C_D is absent and thus the circuit is unilateral. At each bias point in the saturation region, this model may be obtained from

0018-9480/80/0100-0001$00.75 ©1980 IEEE

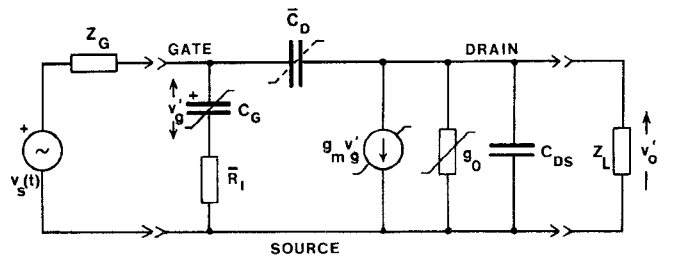

Fig. 1. GaAs MESFET large-signal circuit Model A.

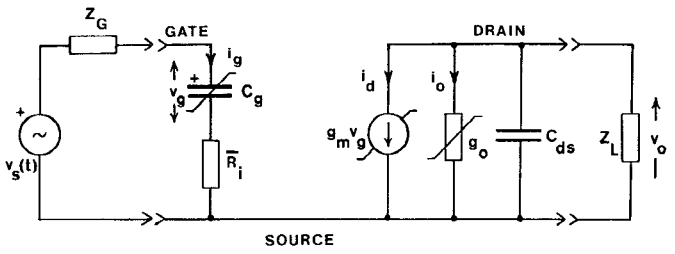

Fig. 2. Simplified nonlinear Model B for MESFET amplifier.

Model A by using the relations given in Fig. 3(a) which partially account for the effects of C_D on the input, output, and forward parameters. Model B can represent MESFET behavior up to frequencies at which feedback becomes significant. The accuracy limits of this approximation for a 2-μm gate-length MESFET are displayed in Fig. 3(b), which compares model-predicted s-parameters with measurements. Similar results apply to other bias points. Predictions based on Model A follow measured parameters to frequencies of 4.5 GHz, whereas the simplified model provides an adequate representation to 3 GHz. In the case of a 1-μm gate-length MESFET, Model A was shown to be in good agreement with measurements to 10 GHz [15], and Model B would be adequate to around 8 GHz. Nonlinear Model B, derived as a function of bias, is used to obtain explicit expressions for intermodulation distortion.

C. Nonlinearity Representation

The two GaAs MESFET's used in experiments were a Plessey 2- $\times$360-μm gate FET and an NEC 1- $\times$300-μm gate transistor. The variation of model elements over regions around the operating bias point was directly determined from s-parameter measurements.

The transconductance nonlinearity and the input gate-to-source channel capacitance are principally determined by the gate voltage, which controls the depth of depletion in the MESFET channel. This is shown in Figs. 4(a) and 5(a). The voltage dependence of these characteristics may be represented by power series of form

$$g_m(V_{GS}) = G_{m1} + G_{m2}V_{GS} + G_{m3}V_{GS}^2 \quad (1)$$

$$C_G(V_{GS}) = C_{G1} + C_{G2}V_{GS} + C_{G3}V_{GS}^2. \quad (2)$$

The output conductance is in general a function of gate-to-source voltage and drain-to-source voltage over the saturation region of bias characteristics, and may be analyzed as a two-dimensional no-memory nonlinearity.

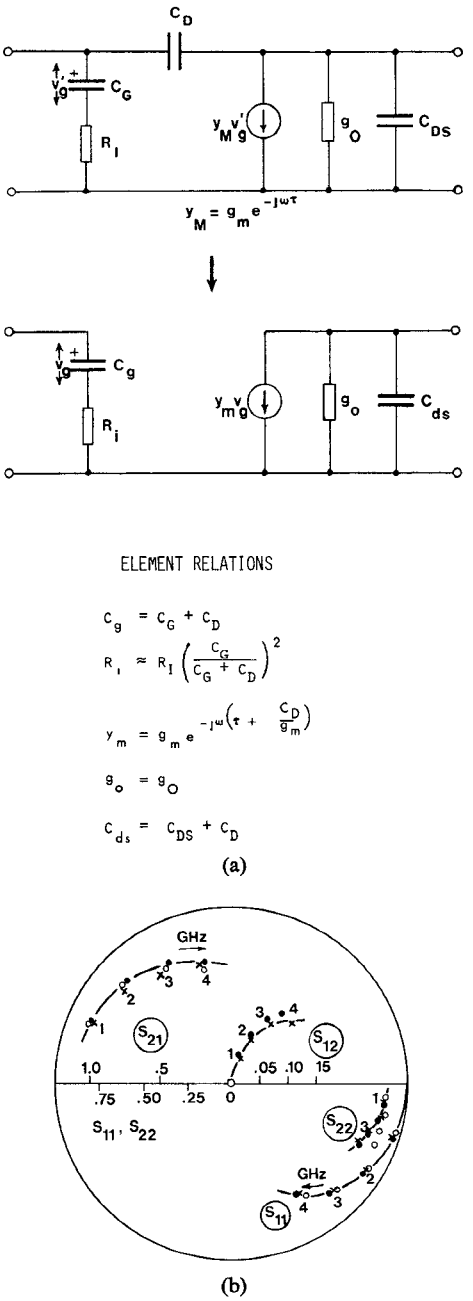

Fig. 3. (a) Element relations for derivation of simplified model. (b) Comparison between model-predicted and measured s-parameters for 2-μm gate MESFET. $\times$ Measured. $\bullet$ Calculated from model including C_D. $\circ$ Calculated from simplified model.

However, for gate voltages corresponding to the high gain amplifier bias conditions, shown in Figs. 4(b) and 5(b), g_0 is primarily dependent on the drain voltage V_{DS} in the saturation region and it was found possible to represent its behavior over this range by a simple expression of the form

$$g_0(V_{DS}) = \frac{a}{(V_{DS}+b)^c}. \quad (3)$$

The feedback capacitance C_D in Model A is a function of drain-to-gate voltage. Its characteristic is shown in Fig. 4(c). For drain voltages in the saturation region ($V_{DS}>$

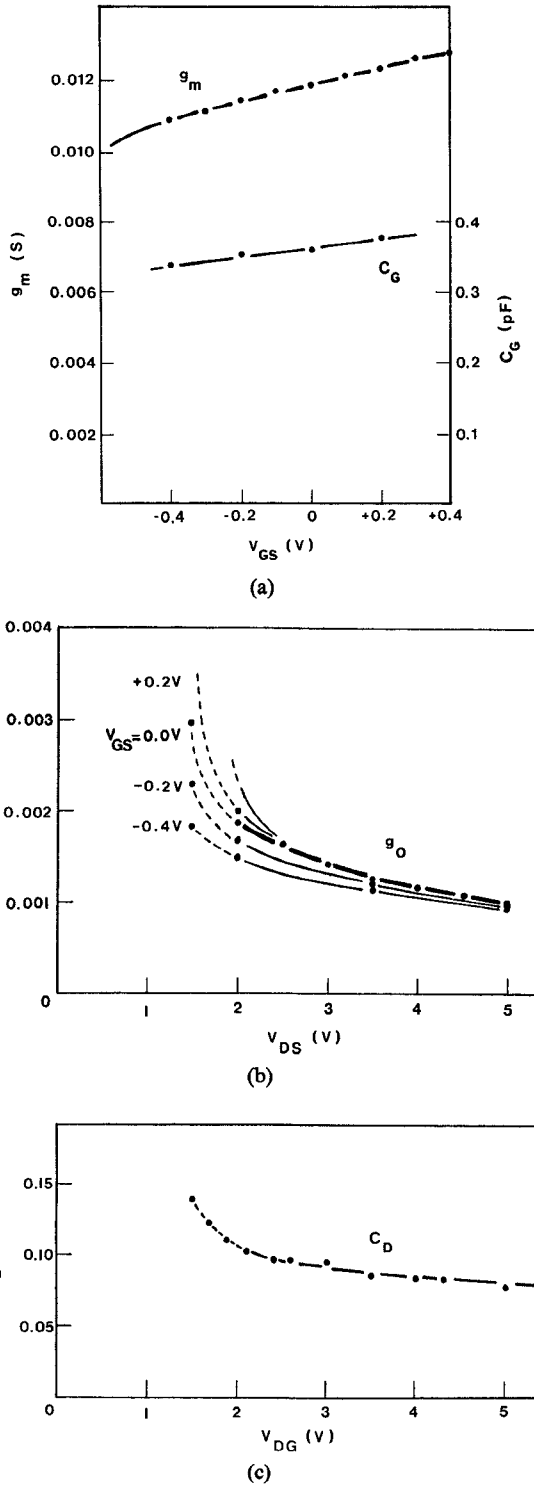

Fig. 4. Nonlinear variation of equivalent circuit elements for 2-μm gate FET. The nonlinear element coefficients refer to (1)–(3). C_{DS} = 0.067 pF, $\bar{R}_I$ = 45 Ω, $\bar{C}_D$ = 0.088 pF. g_m: G_{m1} = 0.012, G_{m2} = 0.0024, G_{m3} = −0.0016. C_G: $C_{G1} = 0.364 \times 10^{-12}$, $C_{G2} = 0.082 \times 10^{-12}$, $C_{G3} \approx 0$. g_0: a = 0.004, b = 0.0, c = 0.94.

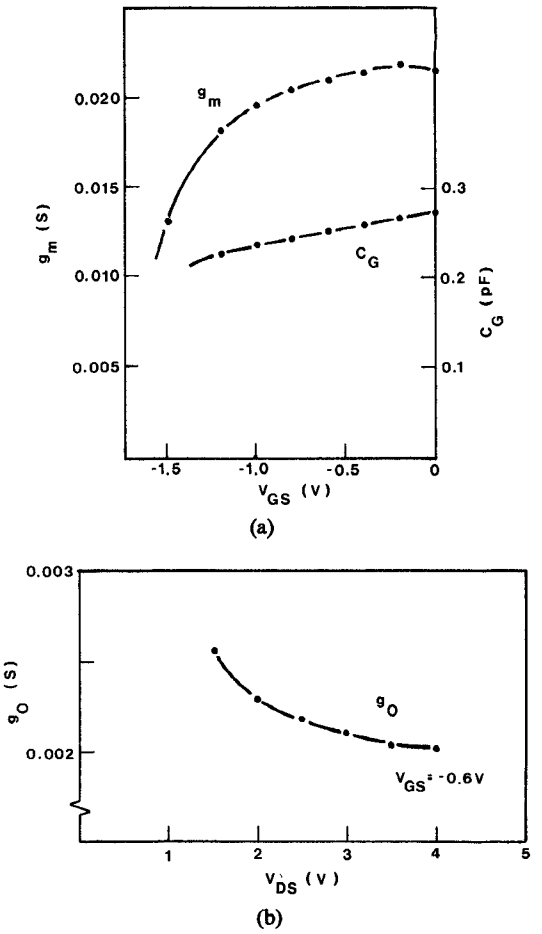

Fig. 5. Nonlinear variation of equivalent circuit elements for 1-μm gate FET. Remaining element values: C_{DS} = 0.06 pF, $\bar{R}_I$ = 12.5 Ω, $\bar{C}_D$ = 0.021 pF.

2 V for this device) the dependence is not strong. The contribution of the nonlinearity to intermodulation distortion was found to be small, thus enabling its averaged value $\bar{C}_D$ to be used in analysis.

The nonlinearities in the model are characterized by least squares fitting of the empirical expressions (1)–(3) to the measured data. Since the distortion predictions are sensitive to the Taylor series coefficients used in analysis, good measurement accuracy is required for their determination (particularly the dominant third degree g_{m3} transconductance coefficient[1]). The nonlinearities are represented as voltage-controlled current generators using a three-term Taylor series expansion of the characteristic about the operating point

$$i_d = \sum_{n=1}^{3} g_{mn} v_g^n \tag{4}$$

$$i_g = \frac{d}{dt} \sum_{n=1}^{3} c_{Gn} v_g^n \tag{5}$$

$$i_0 = \sum_{n=1}^{3} g_{0n} v_{ds}^n \tag{6}$$

where i and v are difference quantities and g_{mn}, c_{Gn}, and

[1]In cases where g_{m3} cannot be evaluated accurately from the transconductance characteristic when the curvature is slight, an additional estimate of its value may be obtained from a measurement of a low-level intermodulation ratio with 50-Ω source and load impedances. The large terminating admittances serve to swamp out the output conductance and input capacitance nonlinearities, thus isolating the transconductance contribution, which may then be readily determined from the IM_3 expression (23) (in Section III) by retaining only the first term.

g_{0_n} are the Taylor series coefficients. The first-order terms in (4) to (6) represent the linear part of the model, whereas the higher order terms in the equations represent the nonlinearities.

III. Nonlinear Analysis

It is assumed that the nonlinear circuit under consideration can be represented by a Volterra series expansion. A sufficient condition for the existence of the Volterra series is that operation of the system is restricted to a region of asymptotic stability [17]. This includes the present amplifier, and enables its output $v_o(t)$ to be expressed in terms of the input signal by the functional series

$$\begin{aligned} v_o(t) = & \int_{-\infty}^{\infty} h_1(\tau) v_s(t-\tau)\, d\tau \\ & + \int\int_{-\infty}^{\infty} h_2(\tau_1,\tau_2) v_s(t-\tau_1) v_s(t-\tau_2)\, d\tau_1\, d\tau_2 \\ & + \int\int\int_{-\infty}^{\infty} h_3(\tau_1,\tau_2,\tau_3) v_s(t-\tau_1) v_s(t-\tau_2) \\ & \cdot v_s(t-\tau_3)\, d\tau_1\, d\tau_2\, d\tau_3 + \cdots \end{aligned} \tag{7}$$

where $h_n(\tau_1,\cdots,\tau_n)$ is the nth-order Volterra kernel, whose Fourier transform $H_n(\omega_1,\cdots,\omega_n)$ is the corresponding nth-order nonlinear transfer function in the frequency domain. In the case of low-distortion amplifiers, the nonlinearities of interest are mild, and hence only the first three terms of the Volterra series are used to characterize the transistor.

With reference to Model B in Fig. 2, the transfer functions (denoted $H_{nc}(\omega_1,\cdots,\omega_n)$) relating the controlling capacitor voltage v_g to the input v_s are obtained as an intermediate step in deriving the transfer functions (denoted $H_n(\omega_1,\cdots,\omega_n)$) relating output v_o to input v_s. Utilizing the techniques described in [18], [19], the first-order transfer functions are found to be

$$H_{1C}(\omega) = \frac{Y_S(\omega)}{Y_i(\omega)} \tag{8}$$

$$H_1(\omega) = -\frac{g_{m1} Y_S(\omega)}{Y_0(\omega) Y_i(\omega)} \tag{9}$$

where

$$Y_S(\omega) = \frac{1}{Z_G(\omega) + \bar{R}_i} \tag{10}$$

$$Y_i(\omega) = j\omega c_{G1} + Y_S(\omega) \tag{11}$$

$$Y_0(\omega) = g_{01} + j\omega C_{ds} + \frac{1}{Z_L(\omega)}. \tag{12}$$

Equations (8) and (9) express the linear response of the circuit in the frequency domain.

The second-order transfer functions are obtained in terms of the first-order functions

$$H_{2C}(\omega_1,\omega_2) = \frac{-j\omega' c_{G2} H_{1C}(\omega_1) H_{1C}(\omega_2)}{Y_i(\omega')} \tag{13}$$

$$\begin{aligned} H_2(\omega_1,\omega_2) = & \frac{-H_{1C}(\omega_1) H_{1C}(\omega_2)}{Y_0(\omega')} \\ & \cdot \left[\frac{-g_{m1} j\omega' c_{G2}}{Y_i(\omega')} + g_{m2} + \frac{g_{02} g_{m1}^2}{Y_0(\omega_1) Y_0(\omega_2)} \right] \end{aligned} \tag{14}$$

where

$$\omega' = \omega_1 + \omega_2. \tag{15}$$

The third-order transfer function for the output is

$$\begin{aligned} H_3(\omega_1,\omega_2,\omega_3) = & -\frac{1}{Y_0(\omega'')} \Bigg[H_{1C}(\omega_1) H_{1C}(\omega_2) H_{1C}(\omega_3) \\ & \cdot \left(g_{m3} - \frac{g_{m1} j\omega'' c_{G3}}{Y_i(\omega'')} - \frac{g_{03} g_{m1}^3}{Y_0(\omega_1) Y_0(\omega_2) Y_0(\omega_3)} \right) \\ & + \overline{H_{1C}(\omega_1) H_{2C}(\omega_2,\omega_3)} \left(-\frac{g_{m1} 2j\omega'' c_{G2}}{Y_i(\omega'')} + 2g_{m2} \right) \\ & + 2g_{02}\, \overline{H_1(\omega_1) H_2(\omega_2,\omega_3)} \Bigg] \end{aligned} \tag{16}$$

where

$$\omega'' = \omega_1 + \omega_2 + \omega_3 \tag{17}$$

and the overbar indicates symmetrization.

Intermodulation is defined for the case of two equal amplitude sinusoid signals at the incommensurate frequencies ω_1 and ω_2 applied to the MESFET input:

$$v_s(t) = V_S \cos\omega_1 t + V_S \cos\omega_2 t. \tag{18}$$

The in-band third-order intermodulation products are generated at frequencies $2\omega_1 - \omega_2$ and $2\omega_2 - \omega_1$.

In terms of the nonlinear transfer functions, the first-order output in Z_L at the fundamental frequency ω_1 is

$$v_{o1} = V_S |H_1(\omega_1)| \cos\left[\omega_1 t + \angle H_1(\omega_1) \right]. \tag{19}$$

The third-order intermodulation output at frequency $2\omega_1 - \omega_2$ is

$$\begin{aligned} v_{o3} = & \tfrac{3}{4} V_S^3 |H_3(\omega_1,\omega_1,-\omega_2)| \\ & \cdot \cos\left[(2\omega_1 - \omega_2)t + \angle H_3(\omega_1,\omega_1,-\omega_2) \right]. \end{aligned} \tag{20}$$

The output power delivered to the load impedance by each spectral component may readily be evaluated from (19) and (20). Third-order intermodulation distortion (IM_3) is defined as the ratio of the distortion output power at $2\omega_1 - \omega_2$ to the fundamental frequency or desired signal power at ω_1 in the load. The important case corresponding to practical two-tone measurements of amplifiers occurs when the frequency separation between the two exciting input signals is very small:

$$\omega_1 \simeq \omega_2 \triangleq \omega. \tag{21}$$

Then the load seen by the fundamental signal and the distortion product ($2\omega_1-\omega_2\simeq\omega$) is virtually the same, and IM_3 may be expressed in terms of the amplifier transfer functions:

$$IM_3=20\log\left[\tfrac{3}{4}V_S^2\frac{|H_3(\omega_1,\omega_1,-\omega_2)|}{|H_1(\omega_1)|}\right]. \tag{22}$$

Using (8)–(17) in (22), an expression for IM_3 in terms of the MESFET amplifier model parameters can be derived:

$$\begin{aligned}IM_3=20\log\tfrac{3}{4}V_S^2\Bigg|&\frac{Y_S(\omega)}{Y_i(\omega)}\Bigg|^2\left(\frac{g_{m3}}{g_{m1}}\right)\\&+\frac{1}{Y_0(\omega)}\left(\frac{\frac{4}{3}g_{02}g_{m2}}{Y_0(\omega_d)}+\frac{g_{m1}^2}{|Y_0(\omega)|^2}\left(\frac{\frac{4}{3}g_{02}^2}{Y_0(\omega_d)}-g_{03}\right)\right)\\&+\frac{2j\omega c_{G2}}{3Y_i(2\omega)}\left(\frac{2j\omega c_{G2}}{Y_i(\omega)}-\frac{2g_{m2}}{g_{m1}}\right)-\left(\frac{j\omega c_{G3}}{Y_i(\omega)}\right)\\&+\frac{\frac{2}{3}g_{02}}{Y_0(2\omega)Y_0^*(\omega)}\left(\frac{-g_{m1}2j\omega c_{G2}}{Y_i(2\omega)}+g_{m2}+\frac{g_{02}g_{m1}^2}{Y_0^2(\omega)}\right)\Bigg|\end{aligned} \tag{23}$$

where $\omega_d=\omega_1-\omega_2$, the asterisk denotes the complex conjugate, and it is assumed that $Z_G(\omega_d)$ is small as is often required for stability at low frequencies. Equation (23) reveals the influence of device parameters, frequency, and termination admittances on distortion. Intermodulation distortion depends on admittances at the harmonic and difference frequencies as well as at the fundamental frequency. The expression contains terms arising from the third degree nonlinear parameters (g_{m3}, c_{G3}, g_{03}) as well as second degree coefficients (g_{m2}, c_{G2}, g_{02}) which give rise to third-order terms by the interaction of the first and second degree kernels. In practice some simplification of the expression is possible because not all terms are significant. For instance, with the present amplifiers the final (fifth) term in (23) was negligible.

The third-order intercept point P_I is used in normalizing the distortion performance of devices for the purposes of comparison. It is defined as the output power at which the intermodulation distortion component equals the fundamental frequency output, when both are extrapolated linearly (on log scales) from low signal levels. At large signals, in the region of gain compression, these extrapolations may be in error due to higher order effects, and this has been noted for some power MESFET's [20]. However, the concept of intercept point remains useful for describing performance in the range to moderate signal levels and is given by

$$P_I=\frac{2}{3}\frac{\mathrm{Re}[Z_L]}{|Z_L|^2}\frac{|H_1(\omega_1)|^3}{|H_3(\omega_1,\omega_1,-\omega_2)|}. \tag{24}$$

IV. Experimental Verification and Discussion

Tests on two experimental amplifiers were conducted to compare measured distortion characteristics with predictions based on the previous analysis. The FET chips were mounted, grounded source, on beam lead carriers. Coaxial tuners were used to optimize performance and the termination impedances were measured and referred to the active device terminals. Intermodulation tests were done with a calibrated variable power two-tone input signal having negligible IMD and harmonic components, and distortion was monitored on a spectrum analyzer.

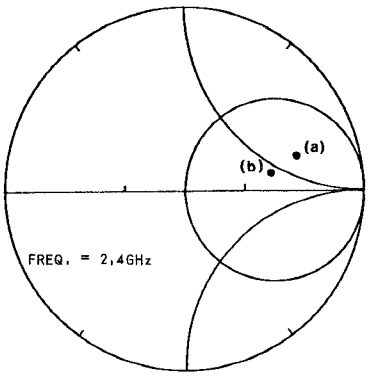

Fig. 6. Experimental load conditions for 2-μm FET amplifier. (a) Maximum gain load. (b) Maximum power load.

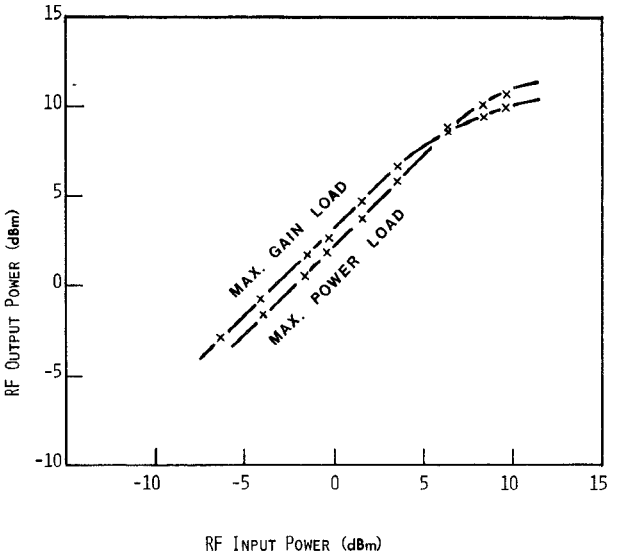

Fig. 7. Single-tone tests on the 2-μm-gate FET amplifier at 2.4 GHz for different load conditions.

The first device tested was a Plessey 2- ×360-μm gate transistor operated at the high gain bias condition of $V_{GS}=0$ V, $V_{DS}=3.5$ V and fed from a 50-Ω signal source. Intermodulation was predicted as a function of input power and frequency. The tuning conditions studied were load impedance for maximum gain corresponding to conjugate matching, and load impedance for maximum output power corresponding to a lower impedance which compromises small-signal gain for increased output power capability.

The measured experimentally tuned impedances (referred to the drain terminal) for the two load conditions at 2.4 GHz are shown in Fig. 6. Results from single-tone tests on the amplifier are given in Fig. 7 and show the effect of the different loads on gain and output power.

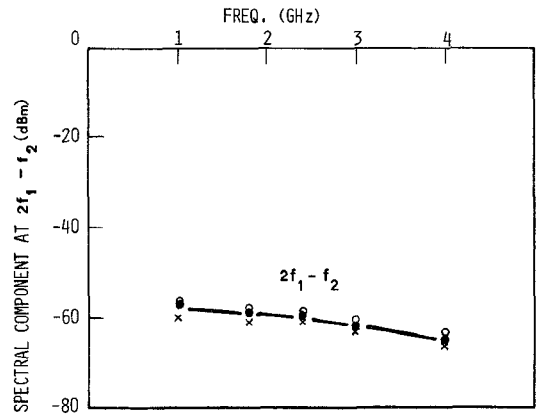

Fig. 8. Measured and calculated frequency dependence of intermodulation distortion for an input of −7 dBm/tone. Amplifier (2-μm FET) terminated in 50 Ω. × Measured. ● Model A prediction. ○ Model B prediction.

Intermodulation distortion was measured by injecting into the MESFET gate two equal amplitude signals separated in frequency by 2 MHz and centered at 2.4 GHz. Results were then compared to two sets of predictions—one based on the Volterra computer analysis of Model A, and the other obtained from closed-form expressions described in the previous section pertaining to Model B.

The frequency dependence of the intermodulation component for the amplifier terminated in 50 Ω is displayed in Fig. 8. It was measured by varying the center frequency of the two-tone input while maintaining frequency separation at 2 MHz. The amplifier fundamental frequency and intermodulation frequency output power as a function of input power per tone at 2.4 GHz is shown for the maximum gain load condition in Fig. 9, and for the maximum power termination in Fig. 10.

The second amplifier employed the higher frequency NEC 1- ×300-μm transistor operated at a bias of $V_{GS} = -0.6$ V, $V_{DS} = 3$ V and fed from a 50-Ω signal source. Care was needed to avoid instability with this device. The load tuning was optimized for high gain and results for the two-tone fundamental frequency component and intermodulation power in the output signal versus input power at 4 GHz are shown in Fig. 11.

Good agreement is seen between the calculated and measured intermodulation characteristics of the amplifiers. Predictions from the simplified Model B compare favorably with measurements, whereas Model A is useful when more accuracy is required for terminations with high reflection coefficients and at high frequencies. The distortion measurements encompass a range from small signals to the gain saturation region. The third-order Volterra analysis predicts a 3 : 1 slope for the intermodulation component versus input power. Deviations from this slope are due to contributions from fifth- and higher order transfer functions (omitted in the present analysis) which become effective at high signal levels. This is evidenced by the changing slope of the intermodulation characteristic in the saturation regime. However, for lower signal levels, Figs. 9–11 display a 3 : 1 slope, indicating that the third-order Volterra analysis applies up to the onset of gain saturation.

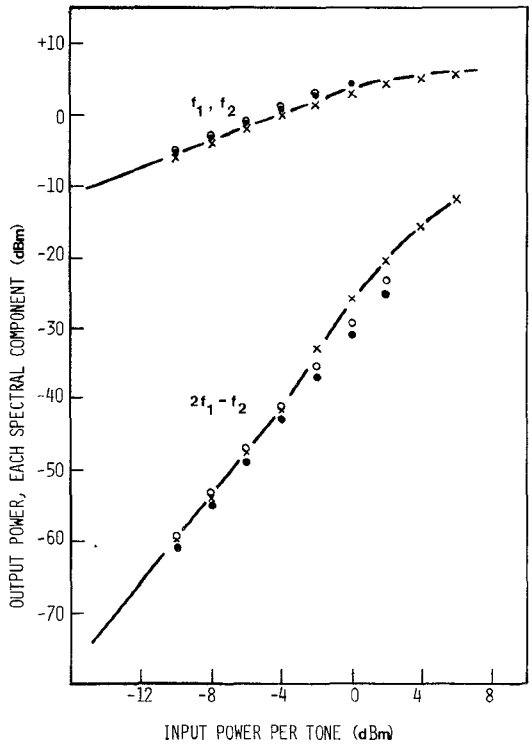

Fig. 9. Measured and predicted fundamental output and IM distortion at 2.4 GHz for a 2-μm FET amplifier with maximum gain load. × Measured. ● Model A prediction. ○ Model B prediction.

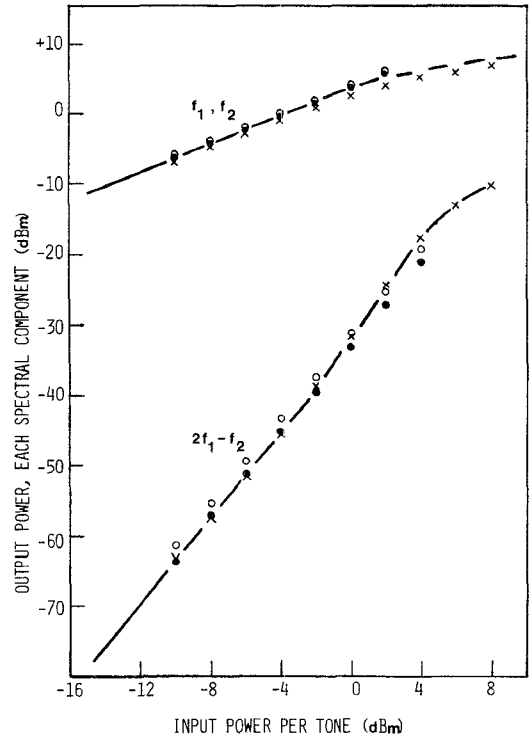

Fig. 10. Measured and calculated fundamental output and IM distortion at 2.4 GHz for 2-μm FET amplifier with load for maximum power. × Measured. ● Model A prediction. ○ Model B prediction.

Having taken into account the interaction between nonlinear parameters (to third degree) and terminating impedances at fundamental, harmonic, and difference frequencies, it is useful to examine the dominant contribu-

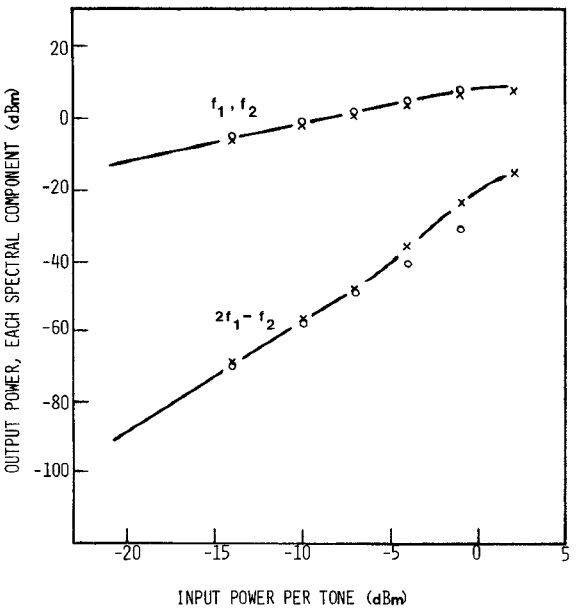

Fig. 11. Measured and predicted fundamental output and IM distortion at 4 GHz for 1-μm FET amplifier with maximum gain load. × Measured. O Model B prediction.

tions to distortion. Table I gives the values of the five terms in the expression for intermodulation (23). This refers to the 1-μm FET, tuned at both source and load to achieve a gain of 16 dB at the 4-GHz fundamental frequency. For low distortion, the harmonic source impedance is taken as 50 Ω (the effect of out-of-band terminations is further discussed below). From Table I, terms in order of significance are Term 1, relating to the g_{m3} coefficient; then Term 2 relating to the output conductance nonlinearity and fundamental frequency load admittance; then Term 3 relating to second degree input nonlinearities and harmonic source admittance. Contributions from the remaining two terms are small (neglecting them results in considerable simplification of (23)).

An important means of controlling distortion is by reducing nonlinearities through device parameter design. GaAs MESFET's with graded channel doping profiles have shown good promise for improving linearity performance [21]. This technique as applied to a practical doping profile design to decrease the third-order g_{m3} and c_{G3} coefficients was investigated in [14]. It is also necessary to consider the effect of the remaining second degree coefficients because they also contribute to third-order distortion by interaction of the first and second degree Volterra kernels. For a complete analysis, the relation between profile grading and all nonlinearities (particularly the drain conductance) is required, and work to this end is under way using numerical computer simulations and charge control. However, under the simplest assumption that the cubic doping profile proposed in [14] makes $g_{m3} = c_{G3} = 0$, with all other parameters unchanged, the present analysis indicates that 8.3-dB improvement in intermodulation ratio is possible. It is noted, however, that this improvement is dependent on the second harmonic source impedance—if it is made 70 jΩ (instead of 50 Ω) the improvement available reduces to 4.8 dB because the

TABLE I
VALUE OF TERMS IN (23)

Term	Value
1	$0.0429/\underline{180^\circ}$
2	$0.023\ /\underline{-167^\circ}$
3	$0.004\ /\underline{171^\circ}$
4	$0.0013/\underline{92^\circ}$
5	$0.0002/\underline{40^\circ}$

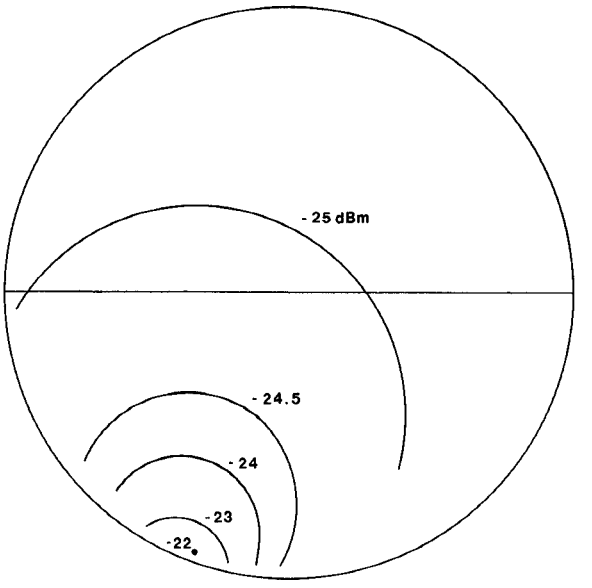

Fig. 12. Contours of constant intermodulation output at 4 GHz versus harmonic source admittance $Y_G(2\omega)$.

contribution from the c_{G2} and g_{m2} coefficients in the third term of (23) becomes large.

Regarding the effect of terminating impedances, the analysis indicates that as the fundamental frequency load admittance is made larger, corresponding to tuning for maximum power output, the intermodulation ratio (at a given input power) decreases. This is indicated by the second term in (23) and corresponds to increased shunting of the output nonlinearity. To investigate the effect of out-of-band terminations, Model A was analyzed with reference to the 1-μm FET and with source and load impedances tuned for 16-dB gain and output of 9 dBm at 4 GHz. The out-of-band terminating impedances were then varied one at a time over the entire stable regions of the Smith chart (with remaining terminations constant). Conclusions (also consistent with Model B) are listed below.

a) Effect of $Y_G(\omega_d)$ was negligible.
b) Effect of $Y_L(\omega_d)$ was small (<1 dB) and is negligible if terminations in the open circuit region of the chart are avoided.
c) Effect of $Y_L(2\omega)$ was small (about 1 dB) which is consistent with measurements [11].
d) Variation of $Y_G(2\omega)$ produced the largest effect on intermodulation. Contours of constant intermodulation output on the source admittance plane (at 2ω) are shown in Fig. 12. A 3-dB variation is observed.

The maximum occurs for a reactive termination which enhances the contribution from the third term in (23).

Sensitivity to the second harmonic source and load impedances were also checked experimentally using a low-pass filter, adjustable length coaxial line combination. Observed sensitivity to the source harmonic termination was greater than to the load harmonic termination. Sensitivity tests, as displayed in Fig. 12, are useful in indicating the range of terminations to be avoided when designing networks to minimize distortion.

V. Conclusion

Intermodulation distortion in microwave MESFET amplifiers has been analyzed using a general Volterra series representation. The analysis takes into account interactions between the nonlinear parameters and generated spectral components. It employs physically based transistor models which are directly determined from small-signal measurements, and enables distortion predictions for realistic circuit embedding conditions. The theoretical intermodulation characteristics showed good agreement with experiments on practical amplifiers. A closed-form expression for third-order IMD ratio was derived which enabled the identification of the major sources of distortion. The analysis was also useful in investigating the effects of the nonlinear parameters and the sensitivity of distortion to source and load terminations at fundamental, harmonic, and difference frequencies. Evaluation of intermodulation is fast, may readily be extended to multistage amplifiers, and should find application in the analysis and design of low-distortion amplifiers.

Acknowledgment

Thanks are extended to D. F. Hewitt for useful discussions.

References

[1] H. Q. Tserng, V. Sokolov, H. M. Macksey, and W. R. Wisseman, "Microwave power GaAs FET amplifiers," *IEEE Trans. Microwave Theory Tech.*, vol. MTT-24, pp. 936–943, Dec. 1976.

[2] D. A. Cowan, P. Mercer, and A. B. Bell, "Low-noise and linear FET amplifiers for satellite communications," *IEEE Trans. Microwave Theory Tech.*, vol. MTT-25, pp. 995–1000, Dec. 1977.

[3] N. Wiener, *Nonlinear Problems in Random Theory*. New York: Technology Press, 1958.

[4] S. Narayanan, "Transistor distortion analysis using Volterra series representation," *Bell Syst. Tech. J.*, pp. 991–1024, May–June, 1967.

[5] R. G. Meyer, M. J. Shensa, and R. Eschenbach, "Cross modulation and intermodulation in amplifiers at high frequencies," *IEEE J. Solid-State Circuits*, vol. SC-7, pp. 16–23, Feb. 1972.

[6] Y. L. Kuo, "Distortion analysis of bipolar transistor circuits," *IEEE Trans. Circuit Theory*, vol. CT-20, pp. 709–716, Nov. 1973.

[7] S. Narayanan and H. C. Poon, "An analysis of distortion in bipolar transistors using integral charge control model and Volterra series," *IEEE Trans. Circuit Theory*, vol. CT-20, pp. 341–351, July 1973.

[8] A. M. Khadr and R. H. Johnston, "Distortion in high-frequency FET amplifiers," *IEEE J. Solid-State Circuits*, vol. SC-9, pp. 180–189, Aug. 1974.

[9] R. G. Meyer and M. L. Stephens, "Distortion in variable-capacitance diodes," *IEEE J. Solid-State Circuits*, vol. SC-10, pp. 47–54, Feb. 1975.

[10] A. Javed, B. A. Syrett, and P. A. Goud, "Intermodulation distortion analysis of reflection-type IMPATT amplifiers using Volterra series representation," *IEEE Trans. Microwave Theory Tech.*, vol. MTT-25, pp. 729–734, Sept. 1977.

[11] R. S. Tucker and C. Rauscher, "Modelling the third-order intermodulation-distortion properties of a GaAs FET," *Electron. Lett.*, vol. 13, pp. 508–510, Aug. 18, 1977.

[12] T. Kouno, Y. Arai, and H. Komizo, "Analysis of GaAs FET third-order intermodulation distortion," *IECE Jap.*, vol. SSD 76-69, 1977.

[13] J. A. Higgins, "Intermodulation distortion in GaAs FETs," *IEEE Int. Microwave Symp.*, pp. 138–141, June 1978.

[14] R. A. Pucel, "Profile design for distortion reduction in microwave field-effect transistors," *Electron. Lett.*, vol. 14, pp. 204–206, Mar. 16, 1978.

[15] R. A. Minasian, "Simplified GaAs MESFET model to 10 GHz," *Electron. Lett.*, vol. 13, pp. 549–551, Sept. 1, 1977.

[16] R. A. Minasian, "Large signal GaAs MESFET model and distortion analysis," *Electron. Lett.*, vol. 14, pp. 183–185, Mar. 16, 1978.

[17] H. Van Trees, *Synthesis of Optimum Nonlinear Control Systems*. Cambridge, MA: M.I.T. Press, 1962.

[18] E. Bedrosian and S. O. Rice, "The output properties of Volterra systems (nonlinear systems with memory) driven by harmonic and Gaussian inputs," *Proc. IEEE*, vol. 59, pp. 1688–1707, Dec. 1971.

[19] J. J. Bussgang, L. Ehrman, and J. W. Graham, "Analysis of nonlinear systems with multiple inputs," *Proc. IEEE*, vol. 62, pp. 1088–1119, Aug. 1974.

[20] E. Strid and T. Duder, "Intermodulation distortion behaviour of GaAs Power FETs," *IEEE Int. Microwave Symp.*, pp. 135–137, June 1978.

[21] R. E. Williams and D. W. Shaw, "Graded channel FET's: Improved linearity and noise figure," *IEEE Trans. Electron Dev.*, vol. ED-25, pp. 600–605, 1978.